

C. Brondi¹, M. R. Di Caprio¹, E. Di Maio^{1*}, T. Mosciatti², S. Cavalca², V. Parenti², S. Iannace³

¹Dipartimento di Ingegneria Chimica, dei Materiali e della Produzione Industriale, University of Naples Federico II, Naples, Italy

²Dow Italia s.r.l, Polyurethanes R&D, Correggio, Italy

³Institute for Polymers, Composites and Biomaterials, National Research Council, Portici (NA), Italy

Microcellular Thermosetting Polyurethane Foams

Thermosetting polyurethane foams are nowadays produced with typical bubble size, $d > 150 \mu\text{m}$, with plenty of room for improvement towards the cellular structure refinement, to gain, among others, in the thermal insulation performances. We herein report a first example of a microcellular thermosetting polyurethane foam, i. e. with bubble size below $5 \mu\text{m}$, produced via the gas foaming technology. In particular, high-pressure CO_2 , N_2 and their mixtures were utilized as blowing agents: solubilized separately into the polymer precursors, they were brought into a supersaturated state by a pressure reduction to induce the bubble nucleation and growth. To achieve microcellular foams, we made use of a novel two-stage pressure reduction program, concurrent to the polymer curing. The first stage is a pressure quench $O(10^{-2} \text{ s})$ from the saturation pressure to an intermediate pressure to induce the nucleation of a large amount of dense bubbles. The second stage is a slow $O(10^2 \text{ s})$ further pressure decrease to ambient pressure, allowing for a slow bubble growth, designed to reach ambient pressure exactly when the curing reached completion.

1 Introduction

Microcellular foams (with average bubble size, $d < 10 \mu\text{m}$) have proven superior to standard foams ($d > 150 \mu\text{m}$) in terms of structural and functional properties and were introduced in the late 80's (Park et al., 1995). To achieve such small bubbles, supersaturation of the blowing agent (BA) solubilized under pressure has to be rapidly induced, with pressure drop rates $O(10^3 \text{ MPa/s})$, most recently up to 10^5 MPa/s (Tamaro et al., 2016). In this way, bubbles nucleation is favored to bubbles growth and a myriad of small bubbles are formed. Since their introduction, microcellular foams from numerous thermoplastic polymers were produced. Nowadays, the technological push towards fine-celled structures has brought to the development of nanocellular foams ($d < 100 \text{ nm}$), which have proven superior to microcellular foams, especially in thermal insulating performances (Okolieocha et al., 2015).

* Mail address: Ernesto Di Maio, Dipartimento di Ingegneria Chimica, dei Materiali e della Produzione Industriale, University of Naples Federico II, P.le Tecchia 80, 80125 Naples, Italy
E-mail: edimaio@unina.it

CO_2 is the largely preferred BA, as it is considered sustainable and safe, with zero ozone depletion potential and the lowest global warming potential ($= 1$) among known BAs (Randall and Lee, 2003). CO_2 has, in general, suitable solubility at processing pressures $O(10^0 - 10^1 \text{ MPa})$. Other BAs, e. g., N_2 , hydrocarbons, are also utilized, characterized by different solubilities (but also different mutual diffusivities, specific volume, interfacial tension, viscosity, relevant to foaming) with respect to CO_2 (Randall and Lee, 2003), with marked differences in the achievable foam. In particular, typically N_2 has a lower solubility and larger diffusivity than CO_2 , giving denser foams characterized by finer bubble structures. In fact, BAs mixtures have been utilized to optimize/tune foaming, typically achieving densities and morphologies intermediate between those achieved by the single neat BA (Di Maio et al., 2005).

Thermosetting polymer foams are nowadays produced with typical $d > 150 \mu\text{m}$, with plenty of room for improvement. Polyurethane (PU) foams are the product of a polyol and an isocyanate (synthesis reaction). Usually, concurrent to the synthesis reaction, a blowing reaction of isocyanate with water (chemical BA) provides the CO_2 that gradually forms and inflates the bubbles at relatively low pressures (Randall and Lee, 2003). Large efforts were made by companies and scientists to reduce d in PU, for instance by using: i) nucleating agents to nucleate a high number of bubbles (Kang et al., 2009; Lee et al., 2016), ii) surfactants to limit bubble coarsening (Han et al., 2009; Baferani et al., 2018), iii) co-BA recipes to tune the timing of bubble formation and growth (Randall and Lee, 2003) and iv) new mixing technologies to enhance the mechanical work responsible for air entrapment (Fiorentini and Griffiths, 1993). No drastic improvements were achieved, so far, in PU morphologies which seem to be dictated by the air-entrapment process and the scale of the multi-phase morphology thereby produced in the expanding matter.

Recently, a radically new technology (Brondi et al., 2019) was introduced to use gas foaming in PU with the aim of obtaining finer morphologies and boost properties such as thermal insulation. The new technology was designed to adapt a thermosetting polymer to the rapid pressure quench method introduced for thermoplastics. In particular, the rapid pressure quench method works efficiently with thermoplastics as they possess relatively fast $O(10^0 - 10^{-2} \text{ s})$ foam setting mechanisms (crystallization or vitrification); thermosets, instead, solidify after relatively slow curing times $O(10^1 - 10^2 \text{ s})$. In the new technology, after having mixed the high-pressure BA/polyol and/or/isocyanate solutions, a two-stage pressure de-

crease program is utilized: in the first stage (foaming stage I), a rapid pressure quench O (10^3 – 10^4 MPa/s) from the saturation pressure O (10^1 – 10^2 MPa) to an intermediate pressure (p') O (10^0 MPa), was imposed to nucleate a large amount of bubbles; in the second stage (foaming stage II), the growth of the nucleated bubbles is controlled by slowly O (10^{-1} MPa/s) further decreasing the pressure to ambient (p_{amb}). Here, the relatively high p' , attained after the first pressure quench, inhibits premature coalescence by keeping the nucleated bubbles small and far apart from each other. The second (slow) pressure reduction (stage II) allows for the slow bubbles' growth, compatible with the curing kinetics. Two mechanisms contribute to the growth of bubbles nucleated at stage I: i) gas expansion and ii) gas diffusion. In fact, at this stage, CO_2 is present in the two phases of the system, the bubbles and the polymer/ CO_2 solution. When the external pressure is reduced in stage II, the gas contained in the bubbles expands (i) and the gas contained in the solution (supersaturated due to the pressure reduction) diffuses into the existing bubbles (ii). The technology was successfully applied in a PU formulation and utilizing neat CO_2 , with the achievement of fine bubbles ($d = 20 \mu m$), medium-to-low density (150 kg/m^3) foams (Brondi et al., 2019).

In this work, we adopt the two-stage pressure quench technology and the use of BA recipe to achieve the first ever produced microcellular thermosetting polyurethane foam. In particular, CO_2 , N_2 and their mixture were utilized to achieve foams with d as low as $4 \mu m$.

2 Material and Methods

A polyether polyol and a polymeric methylene diphenyl diisocyanate (PMDI) (see Di Caprio et al., 2016; 2018 for details) were supplied by Dow Italia S.r.l. (Correggio, RE, Italy) and used "as received". The catalysts introduced in the formulation were pentamethyldiethylenetriamine and dimethylcyclohexylamine. High purity grade CO_2 (99.95 % pure) and N_2 (99.995 % pure) were supplied by SOL (Naples, Italy).

To perform the foaming attempt, we utilized a novel pressure vessel designed to study the foamability of PUs by physical BAs. The equipment was described in Di Caprio et al. (2017). In a typical foaming attempt, schematized by Fig. 1, polyol and PMDI are loaded in a cylindrical sample holder, kept separate by a rubbery impeller to avoid premature curing, and subjected, at $35^\circ C$, to a CO_2 , N_2 or a N_2/CO_2 80–20 vol/vol mixture saturation pressure, p_{sat} , of 6, 15 or 12 MPa, respectively. After a defined sorption time, necessary to achieve the desired BA sorption level (solubilization in Fig. 1), the impeller is put in rotation, and the reactants are allowed to get into intimate contact for the curing reaction to start (mixing). Then, at a certain degree of curing attained after 12 min (common to all of the BAs), an actuated ball valve is opened for the pressure quench with a characteristic time O (10^{-3} – 10^{-2} s) to a low, intermediate pressure, $p' = 0.67, 1.58$ and 1.25 MPa for CO_2 , N_2 or the N_2/CO_2 80–20 vol/vol mixture, respectively, by evacuating the pressure of the pressure vessel into a known volume tank at a fast pressure drop rate (\dot{p}_I) of O (10^2 MPa/s) (foaming stage I). After a certain degree of curing, X' , at p' for 3 min, the pressure is eventually brought to ambient, p_{amb} , when the curing has attained completion, at a slow pressure drop rate (\dot{p}_{II}) of 0.10, 0.20, 0.15 MPa/min for CO_2 , N_2 or the N_2/CO_2 80–20 vol/vol mixture, respectively (foaming stage II). The foamed samples are finally extracted from the sample holder for characterization. It is worth of note that, in Brondi et al. (2019), authors reported a method to calculate the \dot{p}_{II} of the second stage to get from p' to p_{amb} exactly when curing attains completion, known the other processing parameters, the solubilities (Di Caprio et al., 2016; 2018) and the (retarding) effect of the BA on the curing reaction rate (Di Caprio et al., 2019).

Density measurements were performed according to ASTM D792-13, using an analytical balance (Mettler Toledo, Columbus, OH, USA). The cellular structure of the foams was investigated by using a scanning electron microscope (model S440, Leica, Cambridge, UK).

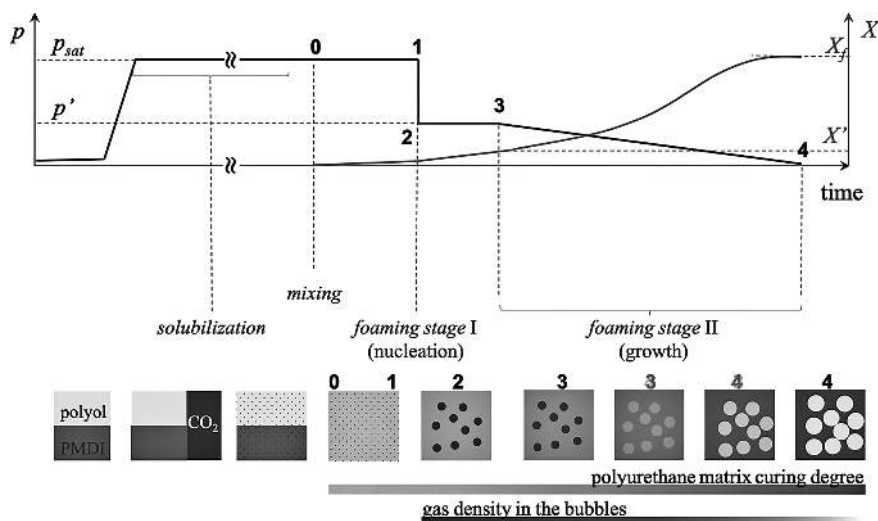


Fig. 1. Scheme of the adopted foaming procedure

3 Results and Discussion

PU samples reported in Brondi et al. (2019) may be considered as the starting point for this work, as we moved forward. In fact, here, microcellular rigid PU foams with smaller bubble size and more uniform bubble morphologies were obtained. The improvement in the PU morphology was achieved by optimizing the processing conditions and adopting other types of BA as well. Figure 2 reports the SEM images of foams produced via one-stage (Fig. 2A, C and E) and two-stage foaming (Fig. 2B, D and F) methods with neat CO₂, neat N₂ and with a N₂/CO₂ 80/20 vol/vol mixture, as BAs. It can be observed that one-stage foamed PU samples presented inhomogeneous bubble morphologies characterized by bi-modal bubble structures. The formation of big bubbles may be attributed to a premature bubbles' nucleation induced by a rapid depressurization on the PU matrix. The nucleated bubbles can grow and merge if the polymer does not possess an adequate viscosity and suitable melt strength to withstand the expansion. The two-stage foaming approach serves to prevent the aforementioned issue. In fact, in the first stage, the rapid depressurization induces the nucleation of a large number density of bubbles, whose expansion is limited by the intermediate pressure, p' . The small bubbles are kept separated by relatively thick walls of the PU network. Subsequent growth is slowly allowed by the later controlled depressurization to ambient pressure. In this way, coalescence is prevented and, as it may be observed from the SEM pictures, extremely fine morphologies were achieved.

The different transport, chemical, and physical properties of the polymer/gas mixture led to different foam morphology in terms of bubble size, foam density and bubble number density (Table 1). For instance, CO₂, with a relatively high solubility in the two precursors (Di Caprio et al., 2016; 2018) even at

moderate pressure of 6 MPa (p_{sat}), gave a low-density foam (130 kg/m³), with average d of ca. 10 μ m. Use of neat N₂ led to better results in terms of bubble size and number density. Despite the higher pressures utilized to foam PUs with N₂ as BA, foam density (440 kg/m³) higher than that of CO₂-blown PU foam was obtained as a consequence of lower solubility. On the other hand, the higher saturation pressures (and the higher \dot{p}_1) led to extremely small average d of 3.5 μ m and higher bubble number density. Finally, the use of a N₂/CO₂ 80/20 vol/vol mixture allowed to obtain a compromise between density reduction and bubble size reduction. As depicted in Fig. 3 reporting the features of the achieved foams, the BA mixture behavior is intermediate between CO₂ and N₂. In this case, the CO₂ fraction in the BAs mixture was enough to inflate the high number of N₂ bubbles generated by the high \dot{p}_1 and to achieve foams with a very fine morphology (d of ca. 5 μ m) and relative low density (245 kg/m³) at the same time.

Use of neat N₂ or of N₂/CO₂ 80/20 vol/vol mixture, due to the lower N₂ solubility into the polymer with respect to CO₂, required the use of larger p_{sat} to attain reasonable density reduction. As the higher the pressure drop rates (achieved by use of the larger p_{sat}) induced high bubble number densities, extremely small bubbles were obtained. When using CO₂, \dot{p}_1 was 36 MPa/s, and the resulting rigid PU foam had a bubble number density of $1.82 \cdot 10^{11}$ #/cm³. As \dot{p}_1 increased, the bubble number density was $5.43 \cdot 10^{11}$ #/cm³ for the N₂/CO₂ 80/20 vol/vol mixture and $6.51 \cdot 10^{11}$ #/cm³ for the neat N₂, with corresponding \dot{p}_1 of 72 MPa/s and 89 MPa/s, respectively. The observed bubble number densities O (10^{11} #/cm³) indicate that a large number of bubbles were successfully nucleated in stage I of the process. In effect, these values are much larger than those typically observed in PUs O (10^6 #/cm³) (Randall, Lee 2003). In addition to the previous comment, one can observe

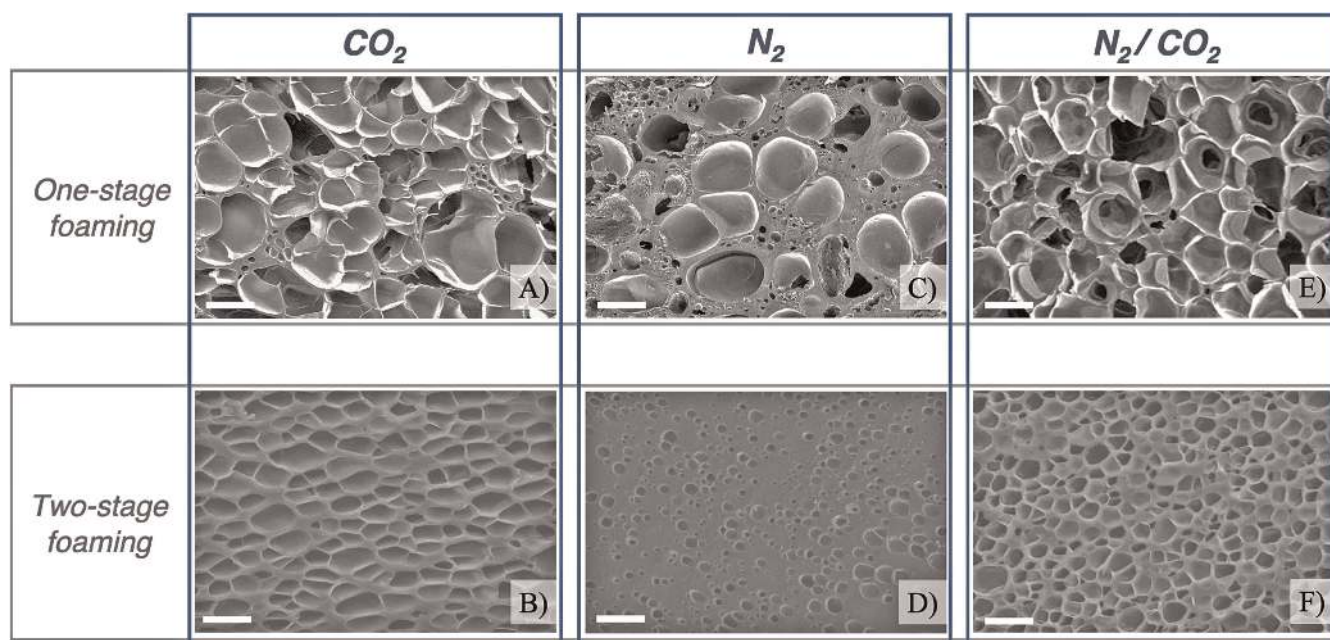


Fig. 2. SEM micrographs of PU foamed by one-stage and two-stage methods with different blowing agents, A), C), E) one stage method, B) D) F) two-stage method; A), B) CO₂, C), D) N₂, E), F) N₂/CO₂ 80/20 vol/vol mixture. Scale bars are 20 μ m.

Sample	BA	p_{sat} MPa	t_{0-1} min	Stage I			Stage II			Foam density kg/m ³	Bubble number density #/cm ³
				\dot{p}_I MPa/s	p' MPa	t_{2-3} min	\dot{p}_{II} MPa/min	d μm			
a	CO ₂	6	12	40.2	/	/	/	20.2 ± 6.4	510	6.62 · 10 ⁹	
b	CO ₂	6	12	35.7	0.67	3	0.10	10.1 ± 1.3	130	1.82 · 10 ¹¹	
c	N ₂	15	12	103.7	/	/	/	17.8 ± 8.7	690	9.11 · 10 ⁹	
d	N ₂	15	12	89.5	1.58	3	0.20	3.5 ± 0.8	440	6.51 · 10 ¹¹	
e	N ₂ /CO ₂	12	12	80.3	/	/	/	17.1 ± 2.1	580	8.41 · 10 ⁹	
f	N ₂ /CO ₂	12	12	71.7	1.25	3	0.15	5 ± 0.2	245	5.43 · 10 ¹¹	

Table 1. Processing program and features of the PU foams achieved by one-stage and two-stage foaming methods

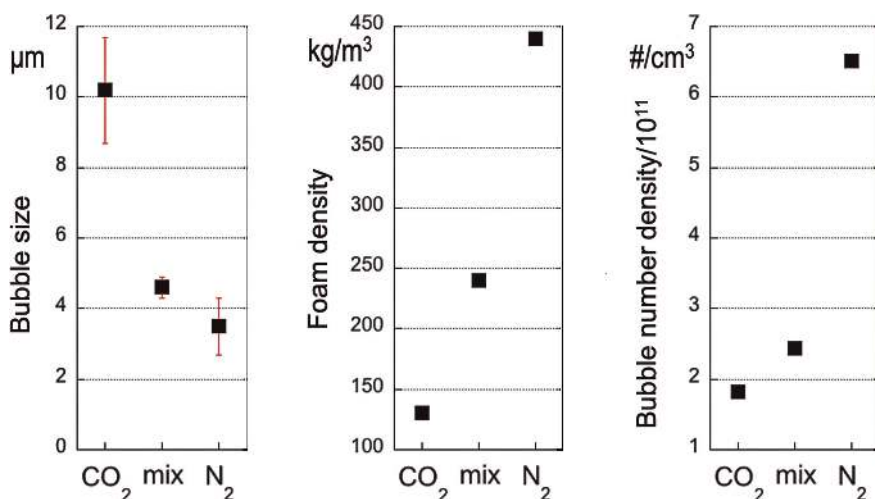


Fig. 3. Features of the PU foams achieved by the two-stage method with CO₂, N₂ and N₂/CO₂ 80/20 vol/vol mixture (mix)

that the nucleated bubbles were kept sufficiently small and far apart from each other by p' to hinder premature coalescence. As it could be expected, \dot{p}_{II} increases with p' , as the larger is p' , the larger is the distance to p_{amb} to attain the final curing degree at the end of stage II. Taking into account the aforementioned processing parameters, the pressure reduction rate \dot{p}_{II} can be properly selected in order to allow a suitable polymer expansion and avoid bubbles coalescence.

4 Conclusions

A two-stage gas foaming method was utilized to obtain microcellular thermosetting polyurethane foams. The method, decoupling the nucleation from the growth stage, avoids excessive stress to the curing polymer, in turn allowing the achievement of medium-to-low density foams. An 80/20 vol/vol mixture of N₂ and CO₂ was efficiently utilized as the BA, with an intermediate behavior between neat N₂ and neat CO₂. Average d below 5 μm , with foam densities in the range 130 to 440 kg/m³ were achieved, proving the great potential of the proposed method to achieve high-performance insulating materials.

References

- Baferani, A. H., Keshavarz, R., Asadi, M. and Ohad, A. R., "Effects of Silicone Surfactant on the Properties of Open-Cell Flexible Polyurethane Foams", *Adv. Polym. Tech.*, **37**, 21643 (2018), DOI:10.1002/adv.21643
- Brondi, C., Di Caprio, M. R., Scherillo, G., Di Maio, E., Mosciatti, T., Cavalca, S., Parenti, V., Corti, M. and Iannace, S., "Thermosetting Polyurethane Foams by Physical Blowing Agents: Chasing the Synthesis Reaction with the Pressure", *J. Supercrit. Fluids*, **54**, 104630 (2019), DOI:10.1016/j.supflu.2019.104630
- Di Caprio, M. R., Dal Poggetto, G., Pastore Carbone, M. G., Di Maio, E., Cavalca, S., Parenti, V. and Iannace, S., "Polyether Polyol/CO₂ Solutions: Solubility, Mutual Diffusivity, Specific Volume and Interfacial Tension by Coupled Gravimetry-Axisymmetric Drop Shape Analysis", *Fluid Phase Equilib.*, **425**, 342–350 (2016), DOI:10.1016/j.fluid.2016.06.023
- Di Caprio, M. R., Immirzi, B., Di Maio, E., Cavalca, S., Parenti, V., Iannace, S. and Mensitieri, G., "Mass Transport and Physical Properties of Polymeric Methylene Diphenyl Diisocyanate/CO₂ Solutions", *Fluid Phase Equilib.*, **456**, 116–123 (2018), DOI:10.1016/j.fluid.2017.10.018
- Di Caprio, M. R., Tammamo, D., Di Maio, E., Cavalca, S., Parenti, V., Fangareggi, A. and Iannace, S., "A Pressure Vessel for Studying Gas Foaming of Thermosetting Polymers: Sorption, Synthesis and Processing", *Polym. Test.*, **62**, 137–142 (2017), DOI:10.1016/j.polymertesting.2017.06.019

- Di Maio, E., Mensitieri, G., Iannace, S., Nicolais, L., Li, W. and Flumerfelt, R. W., "Structure Optimization of Polycaprolactone Foams by Using Mixtures of CO₂ and N₂ as Blowing Agents", *Polym. Eng. Sci.*, **45**, 432–441 (2005), DOI:10.1002/pen.20289
- Fiorentini, C., Griffiths, A. C. M., U. S. Patent 5665287A (1993)
- Han, M. S., Choi, S. J., Kim, J. M., Kim, Y. H., Kim, W. N., Lee, H. S. and Sung, J. Y., "Effects of Silicone Surfactant on the Cell Size and Thermal Conductivity of Rigid Polyurethane Foams by Environmentally Friendly Blowing Agents", *Macromol. Res.*, **17**, 44–50 (2009), DOI:10.1007/BF03218600
- Kang, J. W., Kim, J. M., Kim, M. S., Kim, Y. H., Kim, W. N., Jang, W. and Shin, D. S., "Effects of Nucleating Agents on the Morphological, Mechanical and Thermal Insulating Properties of Rigid Polyurethane Foams", *Macromol. Res.*, **17**, 856–862 (2009), DOI:10.1007/BF03218626
- Lee, Y., Jang, M. G., Choi, K. H., Han, C. and Kim, W. N., "Liquid-Type Nucleating Agent for Improving Thermal Insulating Properties of Rigid Polyurethane Foams by HFC-365 mfc as a Blowing Agent", *J. Appl. Polym. Sci.*, **133**, 43557 (2016), DOI:10.1002/app.43557
- Okolieocha, C., Raps, D., Subramaniam, K. and Altstädt, V., "Microcellular to Nanocellular Polymer Foams: Progress (2004–2015) and Future Directions – A Review", *Eur. Polym. J.*, **73**, 500–519 (2015), DOI:10.1016/j.eurpolymj.2015.11.001
- Park, C. B., Baldwin, D. F. and Suh, N. P., "Effect of the Pressure Drop Rate on Cell Nucleation in Continuous Processing of Microcellular Polymers", *Polym. Eng. Sci.*, **35**, 432–440 (1995), DOI:10.1002/pen.760350509
- Randall, D., Lee, S., "Chaper 7 Outline of Polyurethane Chemistry", in *The Polyurethanes Book*, John Wiley & Sons, New Jersey, p. 113–126 (2003)
- Randall, D., Lee, S., "Chapter 8 Blowing Agents", in *The Polyurethanes Book*, John Wiley & Sons, New Jersey, p. 127–136 (2003)
- Tammaro, D., Astarita, A., Di Maio, E. and Iannace, S., "Polystyrene Foaming at High Pressure Drop Rates", *Ind. Eng. Chem. Res.*, **55**, 5696–5701 (2016), DOI:10.1021/acs.iecr.5b04911

Acknowledgements

This work was partially funded by EU Life-13 ENV/IT/001238 K12 project.

Date received: January 21, 2020

Date accepted: February 12, 2020

Bibliography
DOI 10.3139/217.3936
Intern. Polymer Processing
XXXV (2020) 3; page 326–330
© Carl Hanser Verlag GmbH & Co. KG
ISSN 0930-777X